Sensors and Actuators B 262 (2018) 938–946

Contents lists available at ScienceDirect

Sensors and Actuators B: Chemical

journal homepage: www.elsevier.com/locate/snb

A hand-held fluorescent sensor platform for selectively estimating green algae and cyanobacteria biomass

Young-Ho Shin [a], Jonathan Z. Barnett [b], M.Teresa Gutierrez-Wing [b,c], Kelly A. Rusch [d], Jin-Woo Choi [a,e,*]

[a] School of Electrical Engineering and Computer Science, Louisiana State University, Baton Rouge, LA, USA
[b] Department of Civil and Environmental Engineering, Louisiana State University, Baton Rouge, LA, USA
[c] School of Renewable Natural Resources, Louisiana State University, Baton Rouge, LA, USA
[d] Office of Research, North Dakota State University, Fargo, ND, USA
[e] Center for Advanced Microstructures and Devices, Louisiana State University, Baton Rouge, LA, USA

ARTICLE INFO

Article history:
Received 21 November 2017
Received in revised form 25 January 2018
Accepted 5 February 2018
Available online 11 February 2018

Keywords:
Fluorescent sensor
Multiple analyte detection
Green algae
Cyanobacteria
Light emitting diode

ABSTRACT

This paper reports a portable fluorescent sensor platform containing multiple excitation light illumination for quantification and differentiation of multiple analytes. The fluorescent sensor platform utilizes: (i) three different wavelengths of light emitting diodes (LEDs) for selectively stimulating target analytes; (ii) a sensitive photodetector for corresponding fluorescence measurements; (iii) a custom-built electronic system for data measurement and storage; and (iv) a compact three-dimensional printed housing for the developed sensor platform. Based on the fluorescent emission pattern obtained from each target analyte, multivariate analytical methods were applied to differentiate one analyte from the other in a mixture of multiple analytes. The fluorescent sensor platform was tested to selectively detect two target phytoplankton species: *Chlorella vulgaris* and *Spirulina*. Fluorescent emission of phytoplankton is caused by stimulation of photosynthetic pigments and is widely utilized to quantify and classify phytoplankton groups. Biomass estimation was therefore conducted by measuring chlorophyll *a* fluorescence emission for green algae (*Chlorella vulgaris*) using blue LED excitation and phycocyanin fluorescence emission for cyanobacteria (*Spirulina*) using amber LED excitation. The results demonstrated the viability of the developed device as a portable generic fluorescence sensor platform for simultaneously detecting various biochemical analytes.

1. Introduction

The need for a portable device that simultaneously detects multiple analytes has become critical in numerous areas such as bioscience, environmental quality control, and clinical diagnosis [1–6]. Among several approaches exist for portable sensor applications in detecting multiple analytes [7–13], fluorescence-based detection is one of the most widely used methods owing to its advantages of high sensitivity, high specificity, and simplicity [14,15]. However, most fluorometric systems are large, expensive, and designed to work in highly specific applications.

In this work, we report the development of a hand-held fluorescence sensor platform that can detect and differentiate multiple analytes using three different excitation illumination sources. Three different light emitting diodes (LEDs) are implemented to selectively stimulate the target analytes in a sample solution. A highly sensitive silicon photomultiplier (SiPM) is adopted to detect low fluorescent emission from the sample. The fluorescent sensor system consists of a liquid crystal display (LCD) module, a data storage unit, optical filters, a microcontroller, and relevant electronic circuits, which are enclosed in a compact three-dimensional (3D) printed housing. A disposable glass micro-vial is easily inserted in the sensor system for sample loading.

To demonstrate the ability of the sensor system to selectively detect multiple analytes, a mixture of two phytoplankton species is utilized in this study: green algae (*Chlorella vulgaris*) and cyanobacteria (*Spirulina*). Recent reports show that co-inoculation of green algae and cyanobacteria promotes the growth rate and lifespan of green algae, thereby increasing biofuel production for renewable energy [16–19]. However, monitoring the population of each species is essential because over-proliferation of cyanobacteria cre-

* Corresponding author at: School of Electrical Engineering and Computer Science, Louisiana State University, Baton Rouge, LA, USA.
E-mail address: choijw@lsu.edu (J.-W. Choi).

https://doi.org/10.1016/j.snb.2018.02.045
0925-4005/

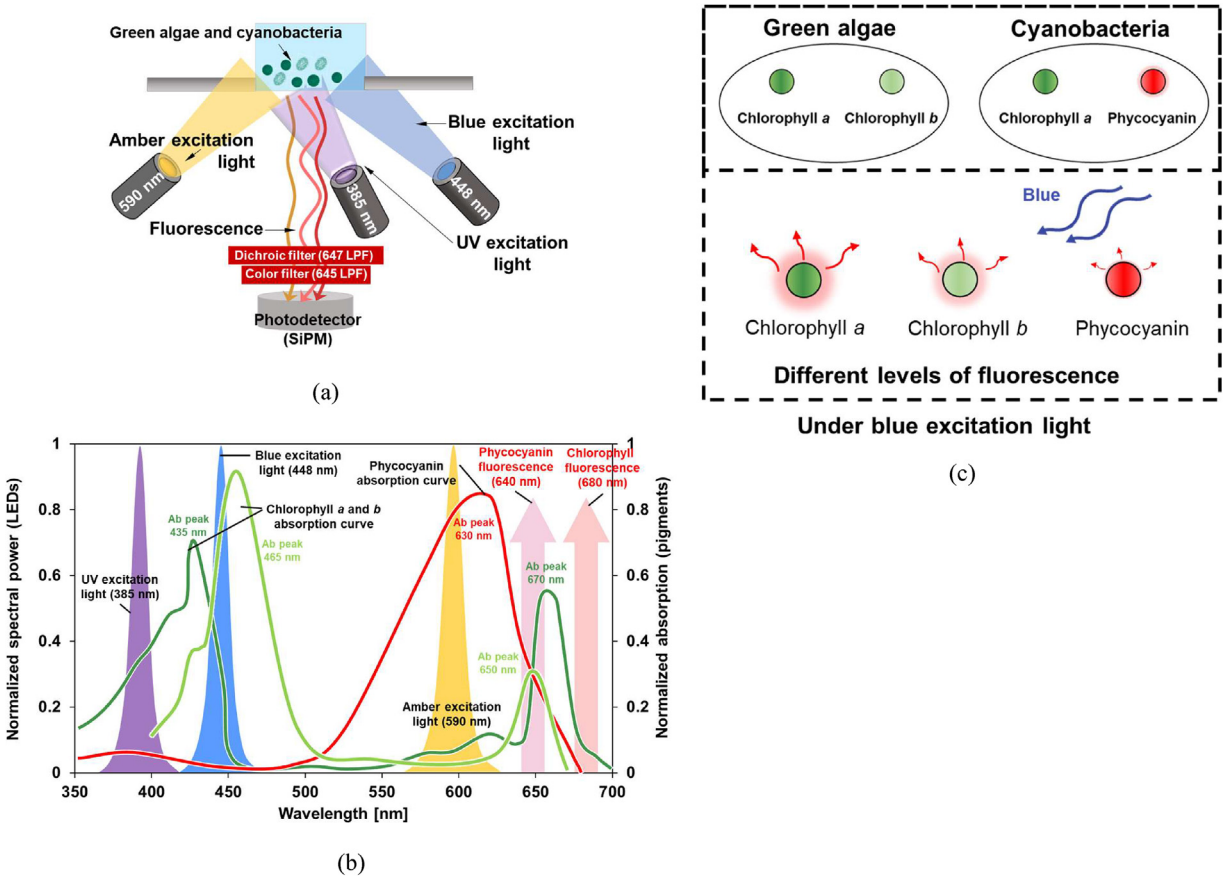

Fig. 1. Working principle of the proposed LED-based fluorescent detection method: (a) schematic illustration of the LED-based fluorescent sensor platform; (b) normalized spectral emissions of excitation LEDs and absorption/emission spectra of photosynthetic pigments, and (c) different molecular excitation levels under the blue light illumination case. (For interpretation of the references to colour in this figure legend, the reader is referred to the web version of this article.)

ates a filamentous layer that lowers biofuel production [20]. Thus, simultaneous monitoring of the populations of green algae and cyanobacteria is desirable to obtain a highly efficient biofuel production system.

In the developed system, to simultaneously detect both phytoplankton species, an *in situ* fluorometry technique is chosen to collect the fluorescent signals of specific pigments in each algal cell. Chlorophyll *a* in green algae and phycocyanin in cyanobacteria are the main photopigments commonly used for detecting individual phytoplankton species [21–25]. The collected corresponding fluorescent signals are analyzed by the multivariate calibration algorithm for differentiation and quantification of each phytoplankton species. Multivariate calibration is a widely used spectroscopic analysis method for estimating the constituent concentrations of analytes when the signals from multiple analytes overlap [26]. Among multivariate analytic methods, including classical least squares (CLS) and principal component regression (PCR), the partial least squares regression (PLSR) method reportedly provides the most accurate biomass prediction estimate for mixed phytoplankton species [27–29]. In this study, we leverage the PLSR algorithm to selectively estimate the biomass of each species using a training sample dataset of fluorescence responses obtained from single and mixed phytoplankton species.

2. Working concept

A schematic illustration of the proposed LED-based fluorescent sensor platform is shown in Fig. 1(a). Color LEDs (Lumileds, CA, USA) with 448 nm (blue) and 590 nm (amber) wavelengths are used to excite the photosynthetic pigments. The blue LED stimulates chlorophyll *a* and *b* photopigments in green algae and emits peak fluorescent light at 680 nm, while the amber LED stimulates phycocyanin photopigment in cyanobacteria and emits peak fluorescent light at 645 nm. An ultraviolet (UV) LED with wavelength 385 nm (Vishay Semiconductor, PA, USA) is employed to stimulate both chlorophyll *a* and phycocyanin for the total phytoplankton measurement. A dichroic mirror (PIXELTEQ, FL, USA) and a color filter (Edmund Optics, NJ, USA) are placed to block the excitation light while selectively allowing the fluorescent signals to pass through it. The corresponding fluorescent emission from each species is collected with a highly sensitive silicon photomultiplier (SiPM) (SensL, Cork, Ireland). An aliquot volume of the sample solution can be easily delivered to the system with a disposable glass micro-vial (0.9 ml, Specialty Bottle, USA).

Fig. 1(b) shows the absorption and emission spectra of different photopigment components and the spectral power distribution of the three excitation LEDs used in our system. Based on the absorption and emission spectra, reabsorption of the phycocyanin fluorescence may also arise from the relatively high absorption rate of chlorophyll around 640 nm. The result of a recent study suggested that the phytoplankton fluorescence conjunction with multivariate analysis is highly effective in predicting chlorophyll *a* concentration from mixed species samples [30]. Therefore, applying a multivariate algorithm should provide an accurate prediction of the sample biomass regardless of any unknown effects. *Chlorella vulgaris* (green algae) has chlorophyll *a* and *b* photopigments, which are primarily stimulated by both blue (448 nm) and UV (385 nm) excitations, but minimally stimulated by amber (590 nm) excita-

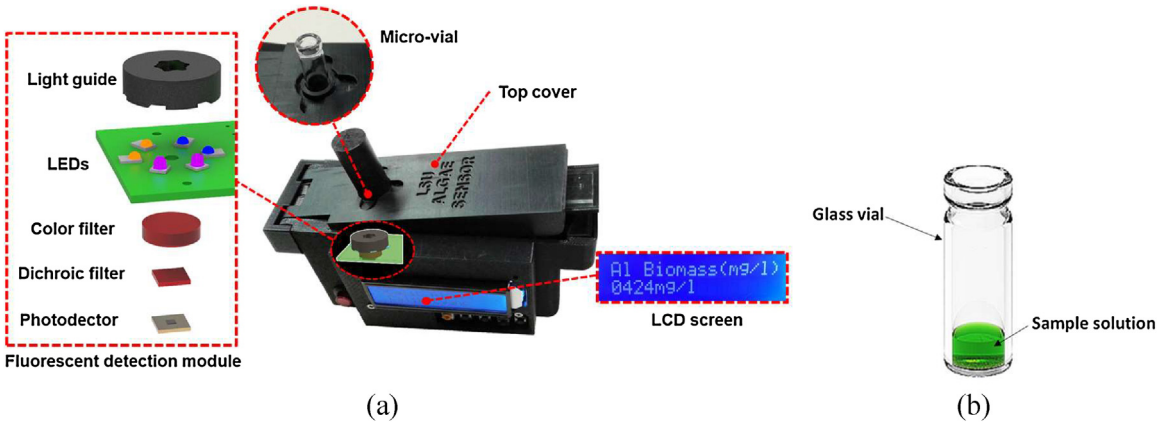

Fig. 2. Photograph and schematics of the fabricated portable fluorescent sensor platform: (a) images of the 3D-printed algae fluorescent sensor with an exploded view of the fluorescent detection module and (b) a glass micro-vial for sample loading.

tion. *Spirulina* (cyanobacteria) contains phycocyanin as the major photosynthetic pigment. It is mainly stimulated by amber excitation, and minimally stimulated by blue excitation.

Simultaneously distinguishing green algae and cyanobacteria is a challenging task because the photopigments in both species are stimulated at the same excitation wavelength. For example, green algae and cyanobacteria both have chlorophyll *a* and measured fluorescence under the blue light excitation, therefore, contains the signals emitted from both species, as shown in Fig. 1(c).

3. Experimental methods

3.1. Sensing system configuration

The portable fluorescent sensor platform, shown in Fig. 2(a), consists of an electronic circuitry, an optomechanical guide, excitation LEDs, an LCD module, a replaceable 9-V battery, and a 3D-printed housing made of a durable plastic material, acrylonitrile butadiene styrene (ABS). Three different wavelengths of surface-mountable LEDs were covered with a 3D-printed optomechanical guide to decrease the reflection noise. The aperture on the printed circuit board (PCB), 3 mm in diameter, was aligned to the central hole of the optomechanical guide and the photodetector window to maximize the fluorescent signal reading. The color filter and the dichroic filter were positioned between the PCB aperture and photodetector window.

The excitation LEDs and the sensing operation were controlled by a custom designed circuitry. The LCD module with selection buttons displays the measurement results, and allows the user to navigate through different menu functions, such as sensor calibration, display of measured results, or loading from the saved data. To easily inject and deliver the sample to the system, a glass micro-vial with a 3D-printed cap blocking ambient light was used (Fig. 2(b)). The top cover was designed to readily accommodate a glass micro-vial and block ambient light when closed.

3.2. Electronic circuitry configuration

The sensor system has three major functional circuitries as shown in Fig. 3(a): an LED-driving circuit, a temperature compensation circuit for the photodetector, and a signal amplification circuit. The LED-driving circuit generates a configurable switching current to control the intensity of each LED while sequentially operating three different wavelengths of excitation LEDs. Each LED set having two identical LEDs coupled in series was turned on for 5 ms and subsequently turned off for 5 ms, and the corresponding fluorescent signals were measured using a photodetector, as illustrated in Fig. 3(b).

The photodetector (SiPM) was biased at −29.5 V for maximum photon sensitivity at room temperature. As the amplification gain of the photodetector varied with both reverse bias and temperature, a high-precision temperature monitoring module was implemented for active gain feedback to maintain a stable gain. The photocurrent collected from the fluorescent signals was amplified with a transimpedance circuit and digitized by the microprocessor at a sampling rate of 2 kHz. The fluorescent readout data were simultaneously displayed on the LCD screen and saved to the onboard storage module. A block diagram of the system functions is illustrated in Fig. 3(c).

3.3. Green algae and cyanobacteria fluorescence detection experiments

For measuring fluorescent signals, glass micro-vials were loaded with different concentrations of green algae, cyanobacteria, and mixed samples. The biomass of *Chlorella vulgaris* (500 mg/l) and *Spirulina* (500 mg/l) samples was initially measured with the dry-weight method. Low biomass concentrations of green algae and cyanobacteria samples were obtained by serially diluting the highest biomass sample stocks.

Experiments were carried out with three replicates of micro-vials for each test. The prepared sample solutions were well agitated using a shaker (Vortex Genie 2, Fisher, USA) before loading them into the micro-vials. After loading the sample solution, the micro-vial was inserted into the sensor system and the cap was affixed to block ambient light. The LEDs were set to emit light intensity of 0.6 $\mu E\,m^{-2}\,s^{-1}$ (or 122 $mW\,m^{-2}$), 0.5 $\mu E\,m^{-2}\,s^{-1}$ (or 109 $mW\,m^{-2}$), and 0.35 $\mu E\,m^{-2}\,s^{-1}$ (or 134 $mW\,m^{-2}$) for the amber, UV, and blue excitation LEDs, respectively.

To apply the PLSR algorithm, a training dataset was collected by measuring the fluorescence from each species and mixed samples of known concentrations. PLSR is a multivariate regression method that correlates one data matrix (fluorescent signal variables, **X**) to another matrix (biomass variables, **Y**). The PLSR algorithm builds a predictive model using correlations between the sample biomass values and the fluorescence signal data. To this end, it decomposes both biomass and fluorescence signal data into eigenvector and score components to identify the most relevant eigenvectors for predicting the biomass of the samples. Four different concentrations of green algae and cyanobacteria sample mixtures were tested in order to validate our predictive model.

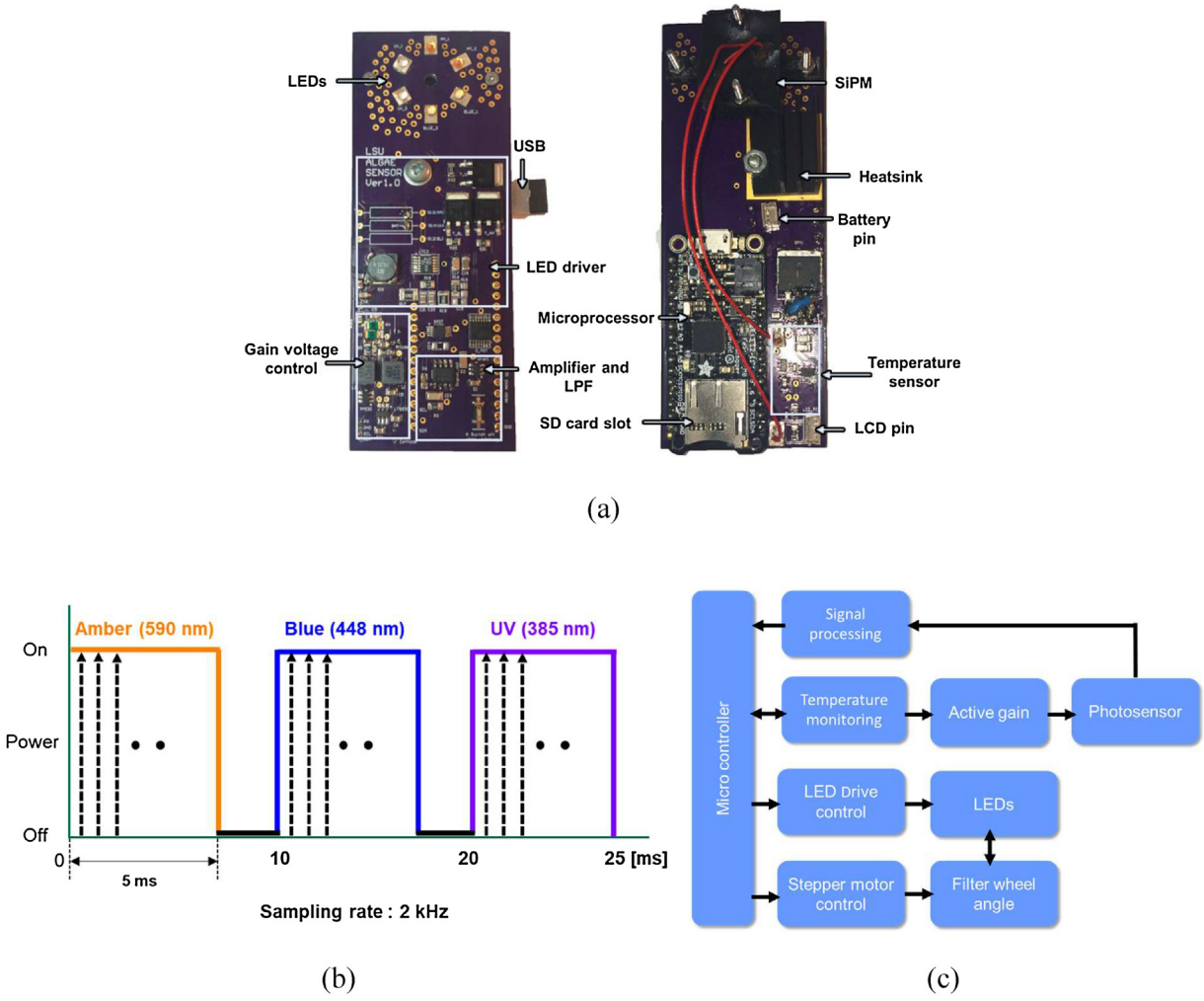

Fig. 3. Electronic circuit design: (a) image of the designed electronic circuit; (b) data acquisition process synchronized with an LED control signal, and (c) block diagram of the circuitry functions.

4. Results and discussion

4.1. Characterization of green algae and cyanobacteria fluorescence

Fig. 4 depicts the fluorescent signal patterns measured with the single species of green algae and cyanobacteria samples (both at a 500 mg/l biomass concentration). The blue line represents the base noise level measured from each excitation LED when tested with a control sample (distilled water). The green line denotes the fluorescent signal pattern when tested with green algae. The green algae signal shows that the blue light excitation induced the highest magnitude of the relative fluorescence value, whereas the amber light excitation induced the lowest fluorescence. This reveals that the blue and UV LEDs successfully stimulated the chlorophyll *a* and *b* components in green algae.

For the cyanobacteria sample, the highest fluorescence response was observed from the amber light excitation in the same graph. The lowest response was from the blue light excitation, which is denoted by orange lines. Thus, the phycocyanin component in the cyanobacteria was successfully stimulated by the amber LED, while chlorophyll *a* stimulation was minimal as discussed in [31]. Moreover, measured fluorescence patterns were used to identify photopigment components of each sample. The obtained unique pattern was also used as a fingerprint for classifying the different phytoplankton groups (green algae and cyanobacteria).

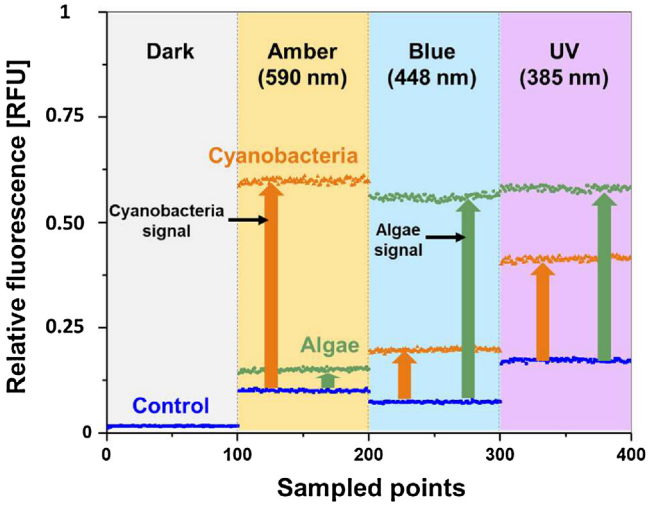

Fig. 4. Different patterns of fluorescence response from green algae and cyanobacteria. (For interpretation of the references to colour in this figure legend, the reader is referred to the web version of this article.)

Fluorescent light intensity of algae decreases under the excitation light over time due to the photochemical quenching effect, which we also observed in our previous work [25]. In order to

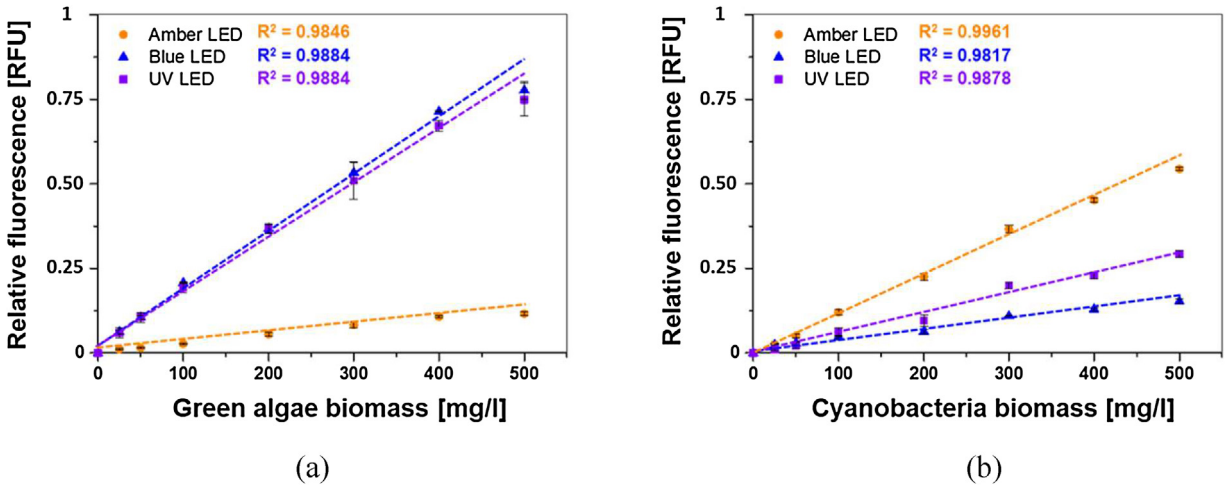

Fig. 5. Measured fluorescence emission from different concentrations of (a) green algae and (b) cyanobacteria using three different excitation LEDs. The error-bars represent the standard deviation of a data set (n = 3).

prevent the cell damage due to the photo bleaching effect on the photopigments, the excitation light intensity of each LED was carefully controlled and maintained at a relatively low level not to damage the cells during experiments. Fig. 4 also shows that the measured fluorescent signals are stable.

4.2. Characterization of green algae and cyanobacteria biomass

A single analyte sample was tested to obtain its calibration curve by plotting the fluorescence emission as a function of the biomass concentration for all three excitation lights. The biomass samples of green algae and cyanobacteria were diluted with distilled water to prepare a series of varying concentration samples. For each analyte, seven different concentrations were prepared and tested: 25, 50, 100, 200, 250, 300, 400, and 500 mg/l. Three replicate measurements were performed for each test, and 100 μl volume of the sample solution was loaded into a micro-vial.

Fig. 5 presents the fluorescence measurement results with different green algae and cyanobacteria concentrations. For the green algae samples, the photocurrent increase was higher with the increasing concentration of the sample under the blue and UV LED lights. Conversely, its change was relatively low under the amber LED light. For the cyanobacteria samples, the photocurrent increase was higher with the increasing concentration of the sample under the amber LED light, while its change was relatively low under the blue and UV LED lights. These measurement results agree well with the fluorescent characteristics of both samples shown in Fig. 4. The lower limit of detection of the developed sensor for the green algae and cyanobacteria were found to be 1 mg/l and 4 mg/l, respectively, according to our experimental results.

4.3. Statistical analysis for identification of green algae and cyanobacteria biomass

The fluorescence signals obtained from the mixture of the two species were also obtained using the sample mixtures listed in Table 1. The acquired data were combined with the results shown in Fig. 5 from single analyte samples to plot all three corresponding fluorescent patterns in 3D space, as illustrated in Fig. 6. Increasing concentrations of green algae show ascending patterns of blue and UV fluorescence while increasing concentrations of cyanobacteria show a corresponding escalation in amber fluorescence for both the single and the mixed analyte samples.

Table 1
Dataset tested for the mixture of two species.

Co-culture sample no.	Biomass (mg/l)	
	Green algae	Cyanobacteria
1	250 (fixed)	0
2	250 (fixed)	25
3	250 (fixed)	50
4	250 (fixed)	150
5	0	250 (fixed)
6	50	250 (fixed)
7	150	250 (fixed)
8	250	250 (fixed)

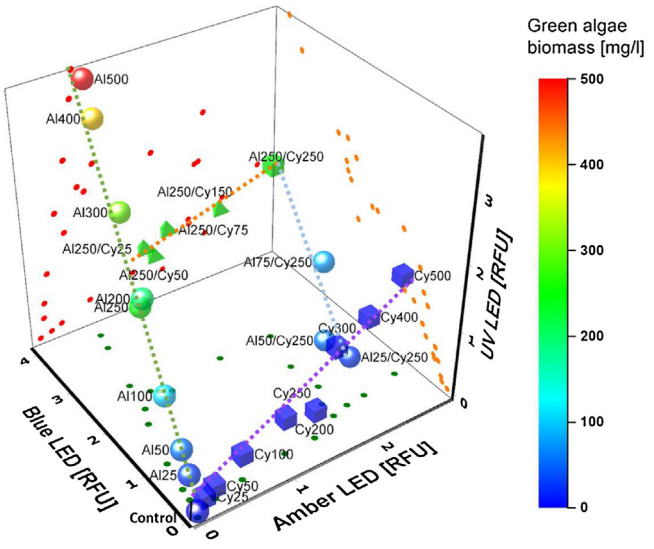

Fig. 6. 3D plot of the measured fluorescent emission from the green algae and cyanobacteria samples for the three different excitation LEDs. (For interpretation of the references to colour in this figure legend, the reader is referred to the web version of this article.)

To simplify the graph, the principal component analysis (PCA) algorithm was employed for easy visualization of the raw data mapped onto the principal component (PC) vector space. The PCs were defined as vectors that best describe a dataset while being represented in lower dimensional space. The PCA algorithm is often used to classify multiple analytes to minimize the redundancy of the raw dataset by linearly reducing the dimensionality [32].

Table 2
Variance of **X**, **Y** and RMSEP described by the components.

Number of coponents	Percentage of described variance for **X**	Green algae biomass ($\mathbf{Y}_1$)		Cyanobacteria biomass ($\mathbf{Y}_2$)	
		Percentage of described variance for $\mathbf{Y}_1$	RMSEP of$\mathbf{Y}_1$ (mg/l)	Percentage of described variance for $\mathbf{Y}_2$	RMSEP of$\mathbf{Y}_2$ (mg/l)
0	0	0	153	0	146
1	62	60	32	60	130
2	99	98	21	98	19
3	100	99	18	99	17

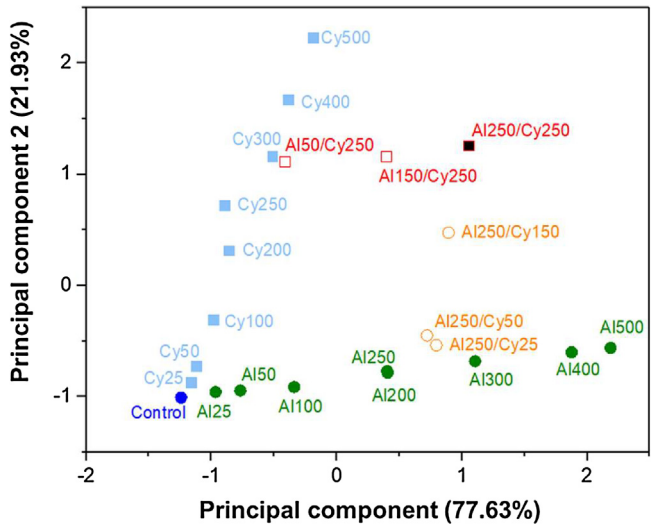

Fig. 7. 2D mapping of fluorescence data measured from the single and the mixed analytes with loadings (PCA bi-plot). The data label beside each point represents the sample species and concentration (mg/l). Al, Cy, and Al/Cy indicate green algae, cyanobacteria, and algae/cyanobacteria mixed sample, respectively. (For interpretation of the references to colour in this figure legend, the reader is referred to the web version of this article.)

Two new coordinates that explain the variation in the dataset were constructed for the first PC (PC_1) representing the direction of the largest variation in fluorescent signal and the second PC (PC_2) correspondingly representing the second largest variation. A dataset matrix of the fluorescence measurement was mapped onto a new two-dimensional score plot space via two base vectors, PC_1 (accounts variance = 77.63%) and PC_2 (accounts variance = 21.93%), as shown in Fig. 7 (total accounts variance = 99.56%). The plot shows that the two PCs are appropriate for separating the sample groups with similar species while describing most of the information from the dataset. Fig. 7 further explains the correlation between the variables. As can be seen, PC_1 is more relevant for explaining the blue and UV fluorescence variables, while PC_2 is more relevant for explaining the amber fluorescence variable. Furthermore, a positive correlation was obtained between the blue and UV fluorescence variables. It is apparent that PCA is an effective qualitative representation method for visualizing different groups of clustered data.

To quantitatively estimate the biomass of the two analytes, the PLSR method was employed for the 23 datasets (fluorescence measurements of 15 single species and eight mixtures of species) measured from three dependent variables (LEDs). The PLSR algorithm extracted the set of components (or latent variables) that accounted for the greatest variation possible in the data while maximizing the covariance of data matrices, **X** (fluorescence measurements) and **Y** (biomass of samples). The component vectors obtained from **X** were then used in the regression step to predict **Y**.

To maximize the accuracy of the predictive model, it is essential to select the optimum numbers of components. This was achieved by evaluating the root mean square error of the prediction (RMSEP) value with different numbers of components. The result is the standard deviation of differences between the predicted and referenced data. The RMSEP is defined as

$$\mathrm{RMSEP} = \sqrt{\frac{1}{N}\sum_{N}^{i=1}(y_i - y')^2}, \quad (1)$$

where N is the number of samples, y is the true biomass, and y' is the predicted biomass. The RMSEP unit is same as that of our prediction values (mg/l). The RMSEP values for both green algae and cyanobacteria changed in accordance with the number of components included for each constructed predictive model. The optimal numbers of components were determined by selecting the minimum RMSEP value for each species. Table 2 shows that the RMSEP value was the lowest with the model of three components for both the green algae and cyanobacteria biomass, indicating that choosing three components gives the lowest prediction error although choosing two components still provides reasonable results.

The dataset matrix was plotted on a new two-dimensional space based on first two components, as shown in Fig. 8. Component 1 accounted for 61% variation in **X** and 60% variation in **Y**, while component 2 accounted for 38% variation in **X** and 39% variation in **Y**. Unlike PCA, the components were selected to maximize the correlation between **X** and **Y** in such a manner that **Y** can be accurately predicted. The PLSR bi-plot shows that the direction of the main variance is different from that of PCA, although the distributions of the dataset are virtually identical in both plots. The blue and UV variables were strongly correlated with the green algae biomass variable, while the amber variable is highly correlated with the cyanobacteria biomass variable. In other words, the fluorescence signals from the blue and UV LEDs were effective in predicting the green algae biomass while fluorescence signals from the amber LED were effective in predicting the cyanobacteria biomass. Thus, when equal amounts of green algae and cyanobacteria are mixed (Al250/Cy250), the direction of the sample vector is centered between the amber and the blue variables.

To evaluate the developed green algae and cyanobacteria biomass predictive model with three components, plots comparing the predicted and the reference biomass were obtained, as shown in Fig. 9. The squares of the correlations for the green algae and cyanobacteria cases were 0.9862 and 0.9794, respectively, indicating that most of the variations in our data were captured by the components in our model. To further validate our model, four different mixtures of green algae and cyanobacteria samples were prepared and blindly tested. The corresponding fluorescent signal data were used to predict the biomass of the mixed species. The mixture concentration for the test and the predicted results are listed in Table 3.

The predicted values show good matching results with an error rate in the range 2–16% of the biomass. The prediction accuracy of PLSR modeling can be improved even more by decreasing the noise. The sources of noise can be device artifacts, measurement errors, and including predictor variables (**X**) that do not explain the prediction values (**Y**). Moreover, including more independent variables that are highly correlated with prediction values will improve the prediction accuracy. In our model, the UV LED is strongly corre-

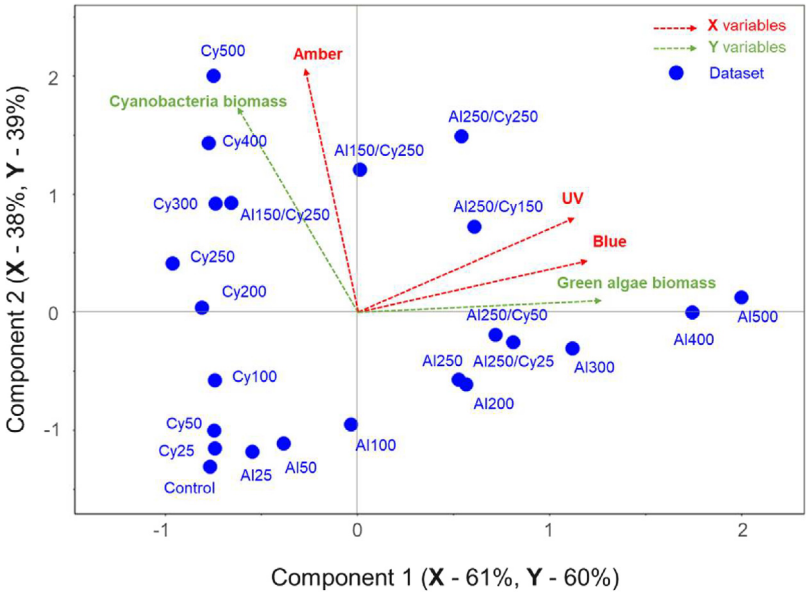

Fig. 8. 2D mapping of fluorescence data measured from the single and the mixed analytes with loadings of **X** and **Y** (PLSR bi-plot). Red dotted lines indicate **X** loadings and green dotted lines indicate **Y** loadings. The data label beside each point represents the sample species and concentration (mg/l). Al, Cy, and Al/Cy indicate green algae, cyanobacteria, and algae/cyanobacteria mixed sample, respectively. (For interpretation of the references to colour in this figure legend, the reader is referred to the web version of this article.)

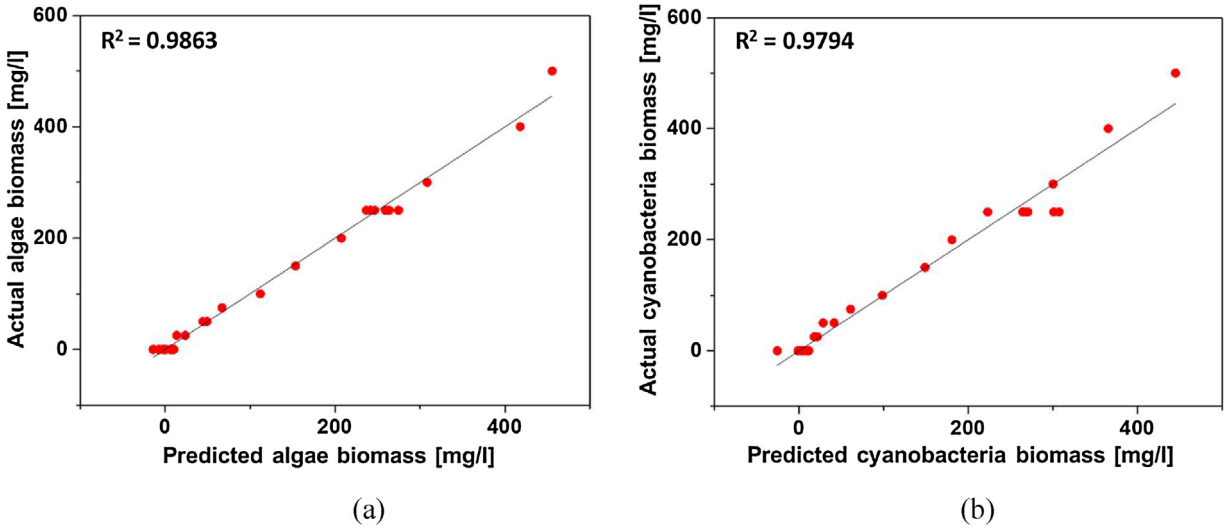

Fig. 9. Predicted vs. reference biomass (mg/l) for (a) green algae and (b) cyanobacteria.

Table 3
Various mixtures of green algae (Y_1) and cyanobacteria (Y_2) samples and estimated biomass.

Test sample no.	Tested biomass [mg/l]		Predicted biomass [mg/l]		Error [%]		Actual deviation [mg/l] (|Test − Predicted|)	
	Y_1	Y_2	Y_1	Y_2	Y_1	Y_2	Y_1	Y_2
1	250	125	238	128	15	2	38	3
2	250	200	246	227	2	14	4	27
3	125	250	118	289	6	16	7	39
4	200	250	186	269	7	8	14	19

lated with the blue LED in explaining the green algae biomass, for which prediction performance was marginally better than that for the two variables (amber and blue LEDs) PLSR model. However, UV LED would be highly useful for differentiating other analytes, especially when it is used in an outdoor environment, such as a lake or a pond, where a color dissolved organic matter (CDOM) is present [33].

5. Conclusions

In this work, a handheld fluorescence sensing platform was developed and demonstrated for selective and quantitative detection of multiple analytes. To demonstrate the efficacy of the developed system, it was used quantify and differentiate two types of phytoplankton species: green algae and cyanobacteria. The green algae were predominantly stimulated by blue and UV LED lights

owing to the presence of chlorophyll *a* and *b*, while the phycocyanin in the cyanobacteria was mainly stimulated by amber LED light. Each LED was sequentially turned on and off using a microcontroller and the corresponding unique patterns of fluorescent signals measured using a highly sensitive photodetector (SiPM) with a long-pass filter. Principal component analysis (PCA) algorithm was used to visualize the clusters of the different sample concentrations. Furthermore, the partial least squares regression (PLSR) algorithm was used to build a predictive model for estimating the biomass of each sample.

The results indicated that the use of different excitation lights was effective in selectively stimulating the target photopigments. Moreover, the application of the PLSR algorithm effectively differentiated and quantified the two algal species. Thus, it is clear that the developed fluorescent sensor system could simultaneously detect multiple analytes. Future improvements to the system will include integration of additional excitation LEDs with various wavelengths for broader spectral stimulation, which will increase the number of detectable analytes of the system.

Acknowledgements

This research was supported in part by Louisiana Board of Regents, Contract LEQSF(2013-2015)-RD-B-02, and National Science Foundation EPSCoR and Louisiana Board of Regents, Contract LEQSF-EPS(2014)-PFUND-347.

References

[1] X.X. Lin, Q.S. Chen, W. Liu, H.F. Li, J.M. Lin, A portable microchip for ultrasensitive and high-throughput assay of thrombin by rolling circle amplification and hemin/G-quadruplex system, Biosens. Bioelectron. 56 (2014) 71–76.
[2] D. Lauwers, A.G. Hutado, V. Tanevska, L. Moens, D. Bersani, P. Vandenabeele, Characterisation of a portable Raman spectrometer for in situ analysis of art objects, Spectrochim. Acta, Part A 118 (2014) 294–301.
[3] Y. Xiang, Y. Lu, Portable and quantitative detection of protein biomarkers and small molecular toxins using antibodies and ubiquitous personal glucose meters, Anal. Chem. 84 (2012) 4174–4178.
[4] W.G. Lee, Y.G. Kim, B.G. Chung, U. Demirci, A. Khademhosseini, Nano/microfluidics for diagnosis of infectious diseases in developing countries, Adv. Drug Deliv. Rev. 62 (2010) 449–457.
[5] C.D. Chin, T. Laksanasopin, Y.K. Cheung, D. Steinmiller, V. Linder, H. Parsa, J. Wang, H. Moore, R. Rouse, G. Umviligihozo, E. Karita, L. Mwambarangwe, S.L. Braunstein, J. van de Wijgert, R. Sahabo, J.E. Justman, W. El-Sadr, S.K. Sia, Microfluidics-based diagnostics of infectious diseases in the developing world, Nat. Med. 17 (2011) 1015–1019.
[6] F.L. Figueroa, C.G. Jerez, N. Korbee, Use of in vivo chlorophyll fluorescence to estimate photosynthetic activity and biomass productivity in microalgae grown in different culture systems, Latin Am. J. Aquat. Res. 41 (2013) 801–819.
[7] B. Rajwa, M.M. Dundar, F. Akova, A. Bettasso, V. Patsekin, E.D. Hirleman, A.K. Bhunia, J.P. Robinson, Discovering the unknown: detection of emerging pathogens using a label-free light-scattering system, Cytom. Part A 77A (2010) 1103–1112.
[8] P. Arora, A. Sindhu, N. Dilbaghi, A. Chaudhury, Biosensors as innovative tools for the detection of food borne pathogens, Biosens. Bioelectron. 28 (2011) 1–12.
[9] A.J. Baeumner, R.N. Cohen, V. Miksic, J.H. Min, RNA biosensor for the rapid detection of viable Escherichia coli in drinking water, Biosens. Bioelectron. 18 (2003) 405–413.
[10] X. Fan, I.M. White, S.I. Shopova, H. Zhu, J.D. Suter, Y. Sun, Sensitive optical biosensors for unlabeled targets: a review, Anal. Chim. Acta 620 (2008) 8–26.
[11] A. Abbaspour, A. Khajehzadeh, A. Ghaffarinejad, A simple and cost-effective method, as an appropriate alternative for visible spectrophotometry: development of a dopamine biosensor, Analyst 134 (2009) 1692–1698.
[12] L. Campanella, A. Bonanni, E. Finotti, M. Tomassetti, Biosensors for determination of total and natural antioxidant capacity of red and white wines: comparison with other spectrophotometric and fluorimetric methods, Biosens. Bioelectron. 19 (2004) 641–651.
[13] J.W. Liu, Y. Lu, A colorimetric lead biosensor using DNAzyme-directed assembly of gold nanoparticles, J. Am. Chem. Soc. 125 (2003) 6642–6643.
[14] L.D. Fricker, L. Devi, Comparison of a spectrophotometric, a fluorometric, and a novel radiometric assay for carboxypeptidase-E (Ec 3.4.17.10) and other carboxypeptidase B-Like enzymes, Anal. Biochem. 184 (1990) 21–27.
[15] S.O. Iseri-Erten, Z.G. Dikmen, N.N. Ulusu, Comparison of spectrophotometric and fluorimetric methods in evaluation of biotinidase deficiency, J. Med. Biochem. 35 (2016) 123–129.
[16] L.E. Gonzalez, Y. Bashan, Increased growth of the microalga Chlorella vulgaris when coimmobilized and cocultured in alginate beads with the plant-growth-promoting bacterium Azospirillum brasilense, Appl. Environ. Microbiol. 66 (2000) 1527–1531.
[17] L.E. de-Bashan, Y. Bashan, M. Moreno, V.K. Lebsky, J.J. Bustillos, Increased pigment and lipid content, lipid variety, and cell and population size of the microalgae Chlorella spp. when co-immobilized in alginate beads with the microalgae-growth-promoting bacterium Azospirillum brasilense, Can. J. Microbiol. 48 (2002) 514–521.
[18] J.J. Tate, M.T. Gutierrez-Wing, K.A. Rusch, M.G. Benton, Gene expression analysis of a Louisiana native Chlorella vulgaris (Chlorophyta)/Leptolyngbya sp. (Cyanobacteria) co-culture using suppression subtractive hybridization, Eng. Life Sci. 13 (2013) 185–193.
[19] J.J. Tate, M.T. Gutierrez-Wing, K.A. Rusch, M.G. Benton, The effects of plant growth substances and mixed cultures on growth and metabolite production of green algae Chlorella sp.: a review, J. Plant Growth Regul. 32 (2013) 417–428.
[20] C. Tamulonis, M. Postma, J. Kaandorp, Modeling filamentous cyanobacteria reveals the advantages of long and fast trichomes for optimizing light exposure, PLoS One 6 (2011) 12, e22084.
[21] D.A. Bryant, Phycoerythrocyanin and phycoerythrin – properties and occurrence in cyanobacteria, Microbiology 128 (1982) 835–844.
[22] H. Zuber, Studies on the structure of the light-harvesting pigment-protein-complexes from cyanobacteria and red algae, Berichte Der Deutschen Botanischen Gesellschaft 91 (1979) 459–475.
[23] E. Gantt, Pigment protein complexes and the concept of the photosynthetic unit: chlorophyll complexes and phycobilisomes, Photosynth. Res. 48 (1996) 47–53.
[24] S.E. Lohrenz, A.D. Weidemann, M. Tuel, Phytoplankton spectral absorption as influenced by community size structure and pigment composition, J. Plankton Res. 25 (2003) 35–61.
[25] Y.-H. Shin, J.Z. Barnett, E. Song, M.T. Gutierrez-Wing, K.A. Rusch, J.-W. Choi, A portable fluorescent sensor for on-site detection of microalgae, Microelectron. Eng. 144 (2015) 6–11.
[26] J. Seppälä, K. Olli, Multivariate analysis of phytoplankton spectral in vivo fluorescence: estimation of phytoplankton biomass during a mesocosm study in the Baltic Sea, Mar. Ecol. Prog. Ser. 370 (2008) 69–85.
[27] G.M. Escandar, P.C. Damiani, H.C. Goicoechea, A.C. Olivieri, A review of multivariate calibration methods applied to biomedical analysis, Microchem. J. 82 (2006) 29–42.
[28] D.M. Haaland, E.V. Thomas, Partial least-squares methods for spectral analyses. 1. relation to other quantitative calibration methods and the extraction of qualitative information, Anal. Chem. 60 (1988) 1193–1202.
[29] L. Moberg, B. Karlberg, Validation of a multivariate calibration method for the determination of chlorophyll a, b and c and their corresponding pheopigments, Anal. Chim. Acta 450 (2001) 143–153.
[30] R. Bhattacharya, C.L. Osburn, Multivariate analyses of phytoplankton pigment fluorescence from a freshwater river network, Environmental Science & Technology 51 (2017) 6683–6690.
[31] L. Dimagno, C.K. Chan, Y. Jia, M.J. Lang, J.R. Newman, L. Mets, G.R. Fleming, R. Haselkorn, Energy transfer and trapping in Photosystem-I reaction centers from cyanobacteria, Proc. Natl. Acad. Sci. U. S. A. 92 (1995) 2715–2719.
[32] M.S. Freund, N.S. Lewis, A chemically diverse conducting polymer-based electronic nose, Proc. Natl. Acad. Sci. U. S. A. 92 (1995) 2652–2656.
[33] Y. Su, F. Chen, Z. Liu, Comparison of optical properties of chromophoric dissolved organic matter (CDOM) in alpine lakes above or below the tree line: insights into sources of CDOM, Photochem. Photobiol. Sci. 14 (2015) 1047–1062.

Biographies

Young-Ho Shin received his B.S. degree in Electrical and Computer Engineering from Kyunghee University, Korea in 2010. He is currently a Ph.D. student in the School of Electrical Engineering and Computer Science at Louisiana State University. His research focuses on the biosensor systems, microfluidic devices, and 3D printing technology. He has been working on developing a portable fluorescent detection system for microalgal samples.

Jonathan Barnett received his B.S. in Environmental Geoscience from Texas A&M University in 2013 and his M.S. degree in Civil Engineering with an emphasis on environmental engineering from Louisiana State University in 2015. While at LSU, he studied the effects of light quality and intensity on a native Louisiana microalgae and Cyanobacteria co-culture. He currently works at Huber Engineered Woods as a Process Safety Engineer.

M. Teresa Gutierrez-Wing received her B.S. in oceanography form the Universidad Autonoma de Baja California (UABC, Mexico), M.S. in oceanography (Marine Ecology) at CICESE, Mexico and PhD in environmental engineering from Louisiana State University (LSU). She performed postdoctoral research at the LSU. Presently, Dr. Gutierrez-Wing is an Assistant Research Professor in the Sea Grant College Program at the Louisiana State University (LSU) and the Aquatic Germplasm and Genetic Resources Center of the School of Renewable Natural Resources in the LSU Agricultural Center in Baton Rouge, LA. Her research interests include microalgae biology, production control and system design, bioproducts extraction and biomass

utilization. Also, the application and use of alternative materials in environmental applications.

Kelly A. Rusch received her B.S. degree in biology and chemistry from the University of Wisconsin-La Crosse in 1986 and her M.S. and Ph.D. in civil engineering from Louisiana State University in 1989 and 1992, respectively. She was a faculty member at Louisiana Staet University from 1993 until 2013 when she left to become the Vice President for Research and Creative Activity at North Dakota State University. Her research background is in automated system design for microalgae and zooplankton culture, decentralized wastewater treatment, industrial waste stabilization and reuse and engineering education.

Jin-Woo Choi received his B.S. and M.S. degrees in electrical engineering from Seoul National University in 1994 and 1996, respectively, and a Ph.D. degree in electrical engineering from the University of Cincinnati in 2001. He joined Louisiana State University in 2003 and is currently a professor in the School of Electrical Engineering and Computer Science at Louisiana State University. His current research activities and interests include biomedical microdevices, point-of-care sensors and systems, nanomaterial-based sensors, bioelectronics, and flexible sensors and wearable devices.